

SCIENTIFIC REPORTS



OPEN

Continuous Flow of Upper Labrador Sea Water around Cape Hatteras

Magdalena Andres¹ , Mike Muglia^{2,3}, Frank Bahr¹ & John Bane³

Six velocity sections straddling Cape Hatteras show a deep counterflow rounding the Cape wedged beneath the poleward flowing Gulf Stream and the continental slope. This counterflow is likely the upper part of the equatorward-flowing Deep Western Boundary Current (DWBC). Hydrographic data suggest that the equatorward flow sampled by the shipboard 38 kHz ADCP comprises the Upper Labrador Sea Water (ULSW) layer and top of the Classical Labrador Sea Water (CLSW) layer. Continuous DWBC flow around the Cape implied by the closely-spaced velocity sections here is also corroborated by the trajectory of an Argo float. These findings contrast with previous studies based on floats and tracers in which the lightest DWBC constituents did not follow the boundary to cross under the Gulf Stream at Cape Hatteras but were diverted into the interior as the DWBC encountered the Gulf Stream in the crossover region. Additionally, our six quasi-synoptic velocity sections confirm that the Gulf Stream intensified markedly at that time as it approached the separation point and flowed into deeper waters. Downstream increases were observed not only in the poleward transport across the sections but also in the current's maximum speed.

The “attached” Gulf Stream—the western boundary current of the wind-driven North Atlantic subtropical gyre—follows the shelf break of the southeastern United States to Cape Hatteras, where it separates abruptly from the continental margin and proceeds to the northeast (Fig. 1). Gulf Stream path deflections and meanders do occur there^{1,2}, but are comparatively small amplitude. Downstream of the Stream's time-varying separation point near $\sim 35.5^{\circ}\text{N}$ ³, path variability is greatly enhanced as the Stream detaches from the steep continental slope and flows into deeper waters⁴.

Near Cape Hatteras, the poleward-flowing Gulf Stream encounters and crosses over the Deep Western Boundary Current (DWBC) which carries waters of the Atlantic Meridional Overturning Circulation's (AMOC's) cold limb equatorward⁵ (blue arrows in Fig. 1a). Both interior and DWBC pathways are thought to play a role in the export of AMOC cold limb waters from the subpolar to the subtropical gyre on its equatorward route⁶. The relative importance of these pathways, their variability, and the mechanisms that drive exchange of these deep waters between the boundary and interior have been the focus of both observational and modeling studies^{7–9}.

Here we discuss a set of recent, high-horizontal-resolution observations of the flows around Cape Hatteras where the DWBC and Gulf Stream have been observed to interact with one another and with the bathymetry^{5,10–12}. Previous studies have shown that the Gulf Stream's detachment latitude may be influenced by the strength of the DWBC here¹³. In addition, those DWBC waters that pass under the separating Gulf Stream in the broad “crossover region” around Cape Hatteras are thought to move to deeper isobaths, conserving their potential vorticity as they continue equatorward along the boundary¹⁴. This area has been a particular challenge for low-resolution climate models to simulate properly as the models tend to produce a Gulf Stream that remains ‘attached’ to the boundary beyond the observed detachment point¹⁵.

On its approach to Cape Hatteras from the Tail of the Grand Banks (i.e., ‘upstream’ of the Cape in a DWBC sense), the DWBC generally lies onshore of the Gulf Stream¹⁶. In this region, the DWBC comprises Upper- and Classical-Labrador Sea Water (ULSW and CLSW)—formed by deep convection in the Labrador Sea—and the denser (and deeper) Overflow Waters formed as Nordic Sea waters spill over the Greenland-Iceland-Scotland sill into the North Atlantic—with these water masses splayed across the slope between the 1000-m and 4000-m isobaths, with the lighter water masses found progressively more onshore and over shallower isobaths. A ten-year record from moorings along Line W south of New England, shows strong transport variability in each of these DWBC components¹⁷ as well as low-frequency property variations in the LSW that can be tied to changes further upstream in the source region⁹. How these transport and property variations are communicated beyond Cape

¹Woods Hole Oceanographic Institution, Woods Hole, MA, 02543, USA. ²University of North Carolina Coastal Studies Institute, Wanchese, NC, 27981, USA. ³University of North Carolina, Chapel Hill, NC, 27599, USA. Correspondence and requests for materials should be addressed to M.A. (email: mandres@whoi.edu)

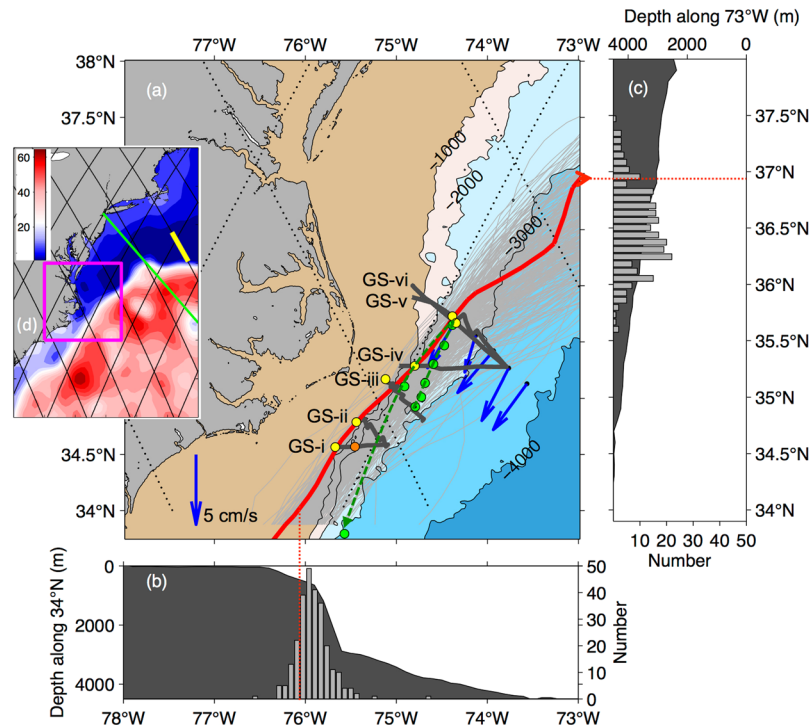


Figure 1. Panel (a) bathymetry around Cape Hatteras (shaded) showing six shipboard ADCP Gulf Stream crossings (dark gray), the ensemble of Gulf Stream paths from monthly-mean 25-cm SSH contours (light gray), the Gulf Stream path during the cruise estimated from the daily altimetry product on 20 April 2017 (red), and an Argo float trajectory (green). Also shown are locations of near-surface (yellow) and one sub-surface (orange) velocity maxima observed on each Gulf Stream crossing. Blue vectors indicate historical mean near-bottom DWBC flow observed with SYNOP moorings⁵. In the velocity sections examined here, the directions of the Gulf Stream velocity maxima at each ADCP crossing are generally well-aligned with the red SSH contour and the ULSW flows are generally well-aligned with the bathymetry. Panel (b) histogram of the longitude of “attached” Gulf Stream paths at 34°N superimposed on bottom topography. Panel (c) analogous histogram for the latitude of the “free” Gulf Stream at 73°W superimposed on bottom topography. Panel (d) regional map with the mapped SSH during the cruise period contoured (cm). The magenta box highlights the area shown in panel (a) and the Line W mooring section (yellow)¹⁷ and the Oleander Line (green)²⁴ are also plotted. The maps in (a) and (d) were generated using Matlab 2014b (Mathworks, Inc.).

Hatteras and into the subtropical gyre (and the role of interior versus boundary pathways in communicating variability between the gyres) remains an area of active research¹⁸. Tracer studies suggest that there must be a DWBC “fast track” that allows some young ULSW (recently ventilated waters with high chlorofluorocarbon concentrations) to flow along the boundary and reach 26°N with little dilution by older interior waters⁷.

Different models and observational techniques have led to different conclusions about how susceptible each DWBC layer is to the detrainment and exchange processes within the crossover region at Cape Hatteras^{11,19,20}. Some of the deepest DWBC waters are observed to cross under the Gulf Stream along the boundary here¹⁰, but as it approaches the crossover region some water is also clearly detrained from the DWBC and flows into the abyssal interior^{11,20,21}. The new observations presented here suggest that some of the lighter DWBC water masses may cross under the Gulf Stream along the boundary more readily than suggested by previous observational studies, which suggested that the lighter DWBC water masses are detrained from the boundary near the Cape.

In one of these previous observational studies, six isopycnal floats from the BOUNCE program in 1994–1995 were deployed within the ULSW layer (~800-m depth) northeast (upstream in a DWBC sense) of Cape Hatteras. These flowed along the boundary towards the crossover region near the Cape²¹. However, none continued to remain on the boundary within the DWBC past the Cape. Rather all were entrained into the separating Gulf Stream and advected eastward away from the boundary. Another study used tracer data and hydrographic sections that were relatively widely spaced around Cape Hatteras. From these, it was surmised¹¹ that none of the shallowest Labrador Sea water ($27.40 \text{ kg/m}^3 < \sigma_0 < 27.73 \text{ kg/m}^3$) passes under the Gulf Stream and that only the onshore-most portion of the deeper Labrador Sea water ($27.73 \text{ kg/m}^3 < \sigma_0 < 27.77 \text{ kg/m}^3$) flows equatorward past Cape Hatteras in a DWBC layer that is continuous around the Gulf Stream’s separation point; the offshore portion of this layer is completely “peeled off” into the interior.

An ongoing study (PEACH: Processes Driving Exchange at Cape Hatteras, funded by the National Science Foundation) is examining the exchange of waters between the continental shelf and open ocean at Cape Hatteras including the influence of the Gulf Stream’s position and strength on the export of shelf waters. Though the DWBC is not a specific focus of PEACH, a cruise in support of PEACH on the *R/V Neil Armstrong* sampled

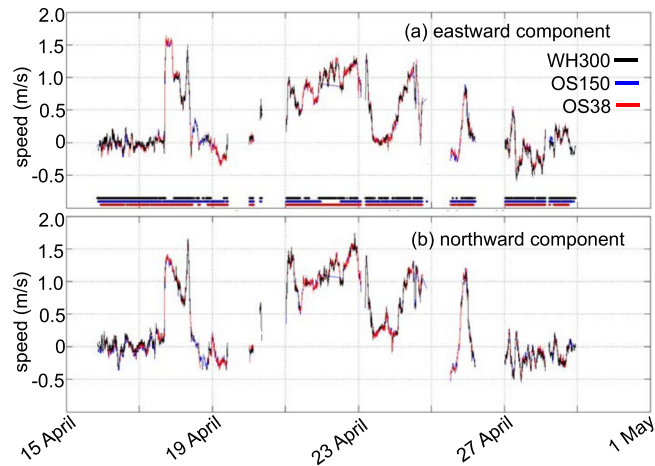


Figure 2. Time series of eastward (a) and northward (b) velocity components for the sonars during the entire AR-15 cruise for the WH300 (black), OS150 (blue), and OS38 (blue). Horizontal lines on (a) indicate the times when the respective ADCP units were returning high quality velocity data.

through the DWBC in April 2017. The cruise spanned the 17-m to 3500-m isobaths on the Middle Atlantic Bight and South Atlantic Bight shelves and the adjacent deeper ocean, where the Gulf Stream transitions from an attached boundary current to a separated flow and encounters the DWBC. Here we report on six Gulf Stream crossings made during this cruise using shipboard acoustic current Doppler profilers (ADCPs). We examine the spatial evolution of the Gulf Stream and a deep counterflow observed in the velocity cross-sections. These velocity data together with observations from conductivity-temperature-depth (CTD) profiles, Argo floats, and satellite altimetry, indicate that there is a continuous path by which even the lightest DWBC water, ULSW, can cross under the Gulf Stream at Cape Hatteras instead of being pulled into the interior. Contrary to the previous studies described above, during our observation period this ‘fast track’ along the boundary was not limited to the most onshore nor the deepest part of the ULSW layer but comprised the entire ULSW layer and at least the top of the CLSW layer.

Data

Shipboard ADCP and CTD. To measure horizontal velocities over a range of depths and vertical resolutions, the *R/V Neil Armstrong* is equipped with shipboard ADCP sonars operating at three frequencies: a Workhorse 300 kHz (WH300), an Ocean Surveyor 150 kHz (OS150) and an Ocean Surveyor 38 kHz (OS38). Vertical and temporal resolutions of the units were set to 2-m bins over 2 minute intervals for the WH300, 4-m bins over 5 minute intervals for the OS150 and 24-m bins over 5 minute intervals for the OS38 with the shallowest bins centered at 10-m, 14-m and 44-m depth, respectively. Concurrently, the ship’s 12 kHz Knudsen echo sounder was run to obtain the collocated bottom depths.

At depths for which there is overlap between the sonars’ bins, the agreement in the measured velocities is excellent. An example is velocity at 68-m depth (Fig. 2), shown for the entire AR-15 cruise (not just the 6 Gulf Stream crossings discussed here). Further details and plots showing the ADCP data from the individual sonars are available at <http://science.whoi.edu/users/seasoar/peachadcp/>. The velocities associated with the barotropic tides are generally weak in the open ocean. To confirm that tidal velocities over the continental slope and abyss off Cape Hatteras are small, we ran the ADCIRC model²² for the southernmost ADCP section (GS_v). Since the tidal contribution to the velocities here is less than 0.1 cm/s (figure not shown), we did not detide the ADCP data for the Gulf Stream sections.

The 38 kHz unit returned high-quality velocity profiles reaching well below the Gulf Stream jet to maximum depths of about 1500-m or to 85% of the full water depth (strong bottom echoes contaminate the deeper bins). Since the approximate bounding depths for the ULSW layer are 750 to 1160 m—with the CLSW layer below this reaching to about 1990 m¹⁷, the shipboard ADCP observations can, in principle, span the whole ULSW layer and top of the CLSW layer. This is confirmed (see below) with hydrographic observations.

Six closely spaced Gulf Stream crossings were conducted between 17 and 25 April 2017 during cruise AR-15 (Fig. 1). Three were continuous sections (GS_v, GS_{iv}, and GS_{ii}), each completed within 3 to 8 hours. The other sections (GS_{ip}, GS_{iii}, and GS_i) were interrupted for full-water-column CTD casts measured with a Sea-Bird Electronics SBE 911plus/917plus CTD, with the deepest reaching 3508 dbar and, in the case of GS_v, to deploy moorings. These sections took 10 to 17 hours to complete except for the most offshore cast on section GS_v, which was taken six days after the rest of that section. GS_{iii} repeated a section collected in 2016 on the *Armstrong*’s first Science Verification Cruise (SVC1) during which evidence of the equatorward flow beneath the Gulf Stream was first noted with the OS38. GS_{iii} is also an extension of a repeat-line along which velocity data have been collected through a companion project (State of North Carolina Renewable Ocean Energy Program: Gulf Stream Observing Group) from a small boat equipped with a 300 kHz ADCP.

	Maximum v_{rot}^1 (m/s)	Ori-entation (°)	Isobath ² (m)	Poleward transp. ³ (Sv)	Maximum v_{eq} (m/s)	Equatorward transp. ⁴ (Sv)	Duration (hrs)	Distance (km)	Start time UTC (d hr:min)
GS _i	1.37 (1.57)	39 (42)	250 (1750)	27.8	0.25	−3.24	3.3	53	21 10:26
GS _{ii}	1.82	30	330	32.2	0.31	−4.31	10.4	50	20 23:56
GS _{iii}	1.92	46	210	33.2	0.24	−2.52	16.2	66	24 12:22
GS _{iv}	1.99	45	—	58.6	0.26	−1.9	4.75	107	23 04:42
GS _v	2.52	55	2300	74.9	0.18	−1.94	16.5	115	17 12:11
GS _{vi}	2.41	39	2390	65.2	0.44 (0.14)	−3.26	8	123	18 04:41

Table 1. Velocities and Transports at the Gulf Stream ADCP sections. ¹Maximum velocity observed in the upper-most bin, which is also usually the overall maximum. For GS_i, the overall maximum, which is also listed (in parentheses), is at 146 m depth. ²Depth over which the maximum v_{rot} is found with data from the ship's 12 kHz echo sounder (except for GS_{iv} when the data were noisy). ³Defined here by the direction of the maximum near-surface velocity. ⁴Defined by the local orientation of the 1000-m isobath: 30° for GS_i through GS_{iv}, and 0° for GS_v and GS_{vi} with the deep-ocean maximum for GS_{vi} given in parentheses.

Argo floats. Four SOLO-II Argo floats (MRV Systems) prepared by the Woods Hole Oceanographic Institution Argo Group were deployed during AR-15. These floats are programmed to initially sample about once per day before beginning their regular 9.9-day mission schedule. Two floats were deployed along GS_v, and one was deployed along GS_{iv}. These were rapidly advected downstream, presumably caught in the deep-reaching Gulf Stream's poleward flow and are not considered further here. The fourth float (SN 7424) was deployed along GS_{iii}, and was first advected downstream by the Gulf Stream during its initial daily sampling schedule (six profiles, green dots in Fig. 1). Thereafter this float was caught in equatorward flow for several of its regular 9.9-day cycles. We argue here that this equatorward flow is the upper part of the DWBC and that this flow can round the Cape, crossing under the Gulf Stream while remaining along the boundary.

Satellite altimetry. Mapped absolute dynamic topography at 1/4° resolution produced from the quality-controlled delayed-time altimetry product, is available through Aviso at daily intervals. Daily maps were averaged to produce monthly SSH maps from 1993 to the end of 2014⁴. Then for each month, the monthly-mean Gulf Stream path is taken to be the 25-cm sea surface height (SSH) contour (Fig. 1, gray curves). Since the delayed-time product is released only at 6-month intervals, the near-real time, daily product is used here to establish the position of the Gulf Stream during the AR-15 cruise (Fig. 1, red curve). From this comparison, it is apparent that the Gulf Stream was approaching the separation point in a relatively on-shore position during the cruise period. To provide additional spatial context for the ADCP sections, we also show the mapped absolute dynamic topography from the time period of the cruise (Fig. 1d).

Results

Using the data described above, we consider the spatial evolution of the velocity structure and transport of the Gulf Stream and the upper part of an observed deep counterflow where these currents navigate one another and the bathymetry around Cape Hatteras.

Spatial evolution of the Gulf Stream. To examine the Gulf Stream, the “poleward” direction is defined here by each section's maximum surface velocity vector. Rotating the ADCP-measured velocity vectors to give downstream (v_{rot}) and cross-stream (u_{rot}) components and integrating over just the areas of positive v_{rot} in each section gives that section's total poleward (Gulf Stream) transport.

During our measurement period, poleward transport increased downstream by more than a factor of two over a downstream distance of only 150 km spanning Cape Hatteras (Table 1). Though this downstream Gulf Stream intensification is consistent with previous studies²³, these transport values may not represent the “throughput” since the sections did not reach offshore to a 0 m s^{−1} isotach. In addition, it is generally difficult to separate transports into the throughput and local recirculations associated with mesoscale eddies that impinge on the offshore edge of the Gulf Stream.

Notably, our April 2017 velocity sections also indicate that Gulf Stream speed increased downstream as the current flowed into deeper water. At the southernmost section, GS_p, the maximum near-surface velocity is 1.4 m/s. At GS_{iv}, the maximum is 2.0 m/s and at the northernmost sections (GS_v and GS_{vi}) the speeds reach ~2.5 m/s. For the three southern sections—GS_i through GS_{iii}, all south of the “separation point”—the location of the maximum surface velocity vector falls between the 210-m and 330-m isobaths. For the “separated Gulf Stream” (i.e., at sections GS_v and GS_{vi}) the maximum surface velocities are found over the 2300 to 2400-m isobaths. Such a local and intense acceleration around Cape Hatteras has not been previously reported for Eulerian nor stream-coordinates time-averages, but is consistent with a 2014 snapshot from quality-controlled CODAR radar data²⁴.

Locations of the near-surface velocity maxima observed with the ADCPs agree remarkably well with the position of the Gulf Stream axis inferred from the 25-cm SSH contour (compare the red curve and yellow dots in Fig. 1). At most sections, Gulf Stream speed is highest in the shallowest ADCP bin (centered at 14-m depth for the OS150). The exception is at GS_i (Fig. 3). Here the near-surface flow (1.4 m/s over the 250-m isobath, yellow vector) is not the strongest; rather the highest speed (1.6 m/s over the 1750-m isobath, orange vector) is found at 146-m depth. As expected, the 25-cm contour tracks the location of the near-surface maximum, not this subsurface maximum (compare the red line and orange dot at GS_i in Fig. 1).

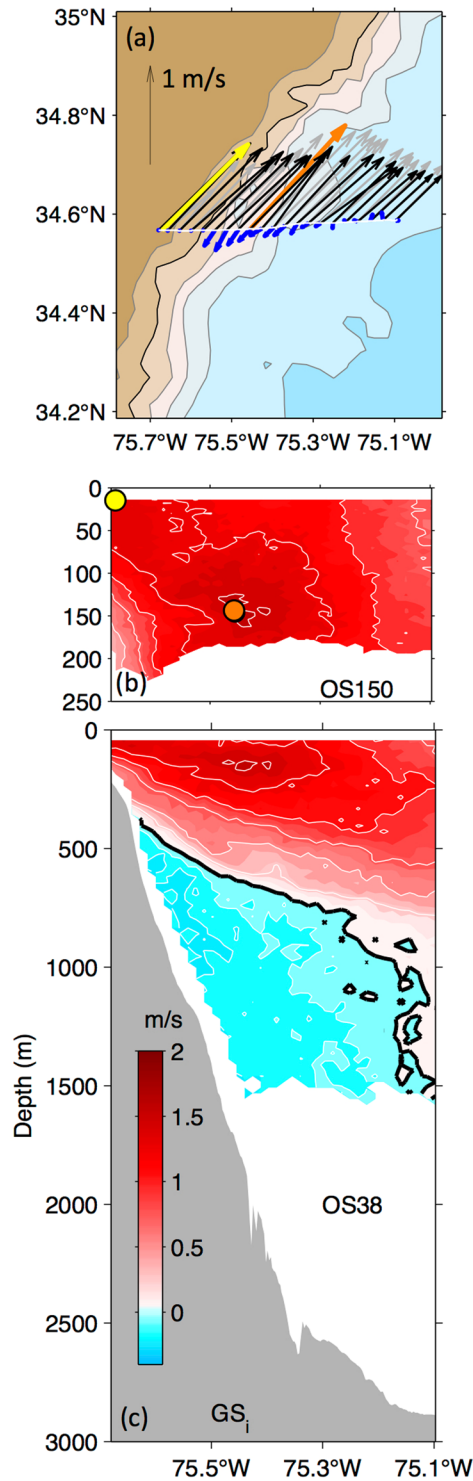


Figure 3. Velocities at GS_i . Panel (a) plan view near-surface (black vectors with maximum highlighted in yellow), at 146-m depth (grey with the section's overall maximum highlighted in orange) and at 980-m depth (blue). Isobaths contoured at 500-m increment (gray) with 1000-m isobath highlighted (black). Panel (b) poleward velocity (v_{rot} , towards 39°) from the OS150. Yellow and orange dots correspond to the colored vectors (a). Panel (c): poleward velocity (v_{rot}) from the OS38 with bottom topography from the ship's underway 12 kHz echo sounder. Black line highlights the 0 m/s isotach. Contour intervals, shown in white, for positive velocities in (b) and (c) are 0.25 m/s and 0.10 m/s for negative velocities. The map in (a) was generated using Matlab 2014b (Mathworks, Inc.).

Spatial evolution of the counterflow. The ADCP data show a deep counterflow beneath the onshore edge of the poleward-flowing Gulf Stream across each of the six velocity sections (Fig. 4). The orientation of the 1000-m isobath, which curves sharply around the Cape, is used to define “equatorward” flow (v_{eq}) at each section.

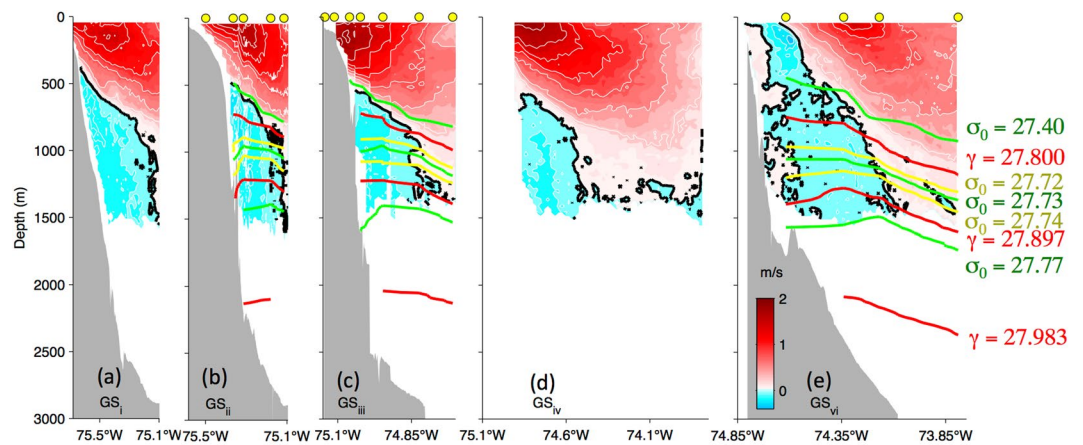


Figure 4. Velocities measured by the OS38 (shaded) rotated to highlight equatorward flow (v_{eq}) across each section with the 0 m/s isotach (black) highlighted and positive velocities (towards 30° for a-d and northward for e) and negative (equatorward) velocities contoured at 0.25 m/s and 0.10 m/s intervals, respectively (white). Green, red and yellow curves highlight isopycnals (kg/m^3) determined from the full-water column CTD casts (locations indicated with yellow dots) taken during the respective ADCP sections. (At GS_{VI} the isopycnals are calculated from casts taken along the same track over the previous 24 hours during crossing GS_{VI}).

In the sections spanning the separated Gulf Stream (GS_V and GS_{VI}), this isobath is roughly meridional and equatorward flow is simply southward ($v_{eq} = -v$, towards 180°). Here v_{eq} is generally less than 10 cm/s (except for a narrow upper-ocean feature, centered at 134-m depth, where v_{eq} reaches 44 cm/s in GS_{VI}). The deep equatorward speeds are consistent with near-bottom DWBC flows observed during the SYNOP program (Fig. 1, blue arrows), where the 7-month means observed between the 2000-m and 4000-m isobaths were about 5 cm/s⁵. Despite relatively low speeds, net equatorward transport captured by the OS38 is substantial since the equatorward flow covers a large cross-sectional area: 1.9 Sv for GS_V and 3.2 Sv for GS_{VI} (Table 1).

South of 35.5°N the 1000-m isobath runs towards 30° and v_{eq} is towards 210°. Once the counterflow rounds the Cape and is squeezed between the Gulf Stream and the steep continental slope here, v_{eq} intensifies. Equatorward speeds at these sections (GS_I through GS_{IV}) exceed 20 cm/s and equatorward transport (integrated where $v_{eq} > 0$) is about 2–3 Sv (Table 1). Since the shipboard ADCP could not measure the deepest velocities (both due to strong interference from bottom returns over the slope and because waters at depths greater than 1500 m are beyond the reach of the OS38), these values represent a minimum bound on the equatorward transport.

Discussion

CTD casts (Fig. 5) suggest that the observed counterflow is the upper part of the equatorward-flowing DWBC. Using water mass definitions based on neutral density, γ ,⁶ from Toole *et al.*¹⁶ the sections' ULSW ($27.800 \text{ kg/m}^3 < \gamma < 27.897 \text{ kg/m}^3$) and CLSW ($27.897 \text{ kg/m}^3 < \gamma < 27.983 \text{ kg/m}^3$) are indicated by the red curves in Fig. 4. These isopycnals slope across the sections and are deeper within the deep-reaching Gulf Stream on the offshore sides of the sections. On the onshore sides—where the counterflow is observed—the OS38 captures the entire ULSW layer and even the upper-most CLSW.

In Pickart and Smethie¹¹ water masses were considered using potential density referenced to the surface, σ_0 (green curves in Figs 4 and 5). They found that none of the lightest Labrador Sea Water (the layer between the widely-spaced green curves on the theta-S plot in Fig. 5b) and only some of the 'intermediate' Labrador Sea Water (between the tightly spaced green curves in Fig. 5b) rounds Cape Hatteras along the boundary. In contrast, our shipboard observations from AR-15 show equatorward flow in *both* density classes (blue dots in Fig. 4b).

Another set of isopycnals shown in Fig. 4 (yellow) depicts the density range within which RAFOS floats were deployed in the BOUNCE program. These floats were ejected in the crossover region²¹. In contrast, the AR-15 velocity sections examined here suggest a smooth, connected flow in this density class. Indeed this impression of a "connected" flow is corroborated by the trajectory of the Argo float which was entrained in the deep flow, nominally at 1000 dbar from the 6th to the 8th satellite fix (Fig. 1a, green dots). With about 10 days between these fixes and 230 km covered by the float, the mean speed experienced by the float in this layer is 27 cm/s, which is remarkably close to the maximum v_{eq} from the ADCP velocity sections (Table 1).

Finally, to provide context for these "snapshot" sections, we consider the 10-year mean equatorward transport observed by the Line W mooring array across the DWBC south of Cape Cod (Fig. 1d, yellow line). Here the mean is 4.33 ± 0.46 Sv for the ULSW layer and 7.37 ± 1.20 Sv for the CLSW layer¹⁷ (reporting their 'average of daily profiles'). Not surprisingly, the AR-15 transports are somewhat lower (1.9–4.3 Sv, Table 1). This may be due in part to the limited reach of the OS38 over topography and may reflect detrainment of some DWBC between Line W and Cape Hatteras (particularly in the ULSW layer).

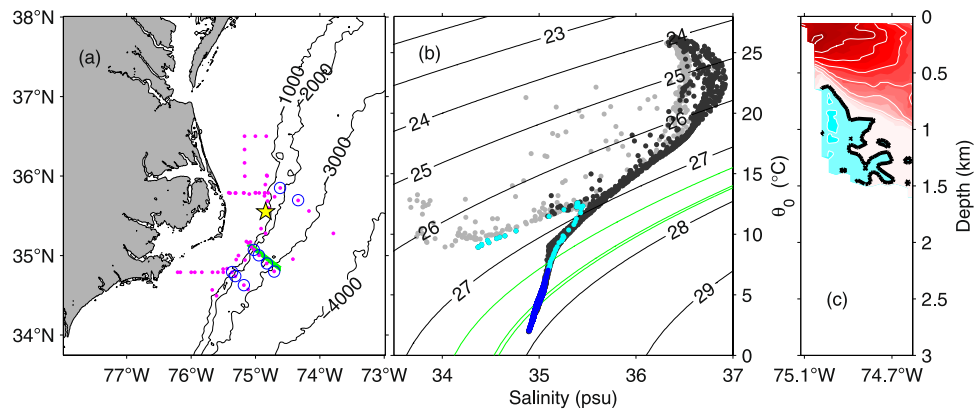


Figure 5. Panel (a) map of CTDs from AR-15 (magenta) with those circled at which equatorward deep flow was observed (blue). Also shown is ‘the Point’ by Hatteras (star), and location of the SVC1 ADCP section (green). Panel (b) theta-S curves for casts over isobaths shallower than 500-m (light gray) and exceeding 500-m (black, blue and cyan) where the blue and cyan dots highlight the portions of these deep-reaching casts where equatorward flow was observed (Fig. 4). The upper 500 m of the cast which sampled through the strong upper-ocean feature noted in section GS_{vi} (Fig. 4e) is shown in cyan. Black lines show σ_0 (kg/m^3) with green lines highlighting shallow ($27.40 \text{ kg/m}^3 < \sigma_0 < 27.73 \text{ kg/m}^3$) and deeper ($27.73 \text{ kg/m}^3 < \sigma_0 < 27.77 \text{ kg/m}^3$) Labrador Sea Water classes of¹¹. The $\sigma_0 = 27.72 \text{ kg/m}^3$ and 27.74 kg/m^3 (yellow lines in Fig. 4) fall almost on top of the central ($27.73 = \sigma_0$) green line. Panel (c) v_{eq} from SVC1 (along green line in a), with shading and contours as in Fig. 4. The map in (a) was generated using Matlab 2014b (Mathworks, Inc.).

Conclusions

Shipboard observations from AR-15 and the Argo float deployed during that cruise, suggest that flow in the DWBC’s ULSW and CLSW layers is continuous along the boundary around the Cape, at least under some circumstances. This is corroborated by the SVC1 cruise in 2016 when a deep counterflow was also observed with the OS38 in the section along GS_{iii} (Fig. 5c). Shipboard data from upcoming cruises and mooring data presently being collected through the PEACH program (<https://sites.google.com/a/ncsu.edu/peach-public-site/home>) will help characterize variability in this crossover region and will provide context for the data presented here so that the underlying dynamics can be investigated further.

Combining shipboard ADCP sonars operating at different frequencies provides a powerful observational tool to characterize the ocean. The 38 kHz unit is making observations of the deep ocean more readily accessible and useful datasets are being built up by the now-routine sampling from vessels in the UNOLS fleet like the *R/V Neil Armstrong*. In addition to the research fleet, ships of opportunity are also collaborating with the research community to outfit commercial vessels with ADCPs^{25,26}. Efforts are underway to equip the *C/V Oleander*, a container ship that makes weekly round trips between New Jersey and Bermuda, crossing the shelf flow, DWBC, Gulf Stream and Sargasso Sea (green track in Fig. 1d), with a 38 kHz ADCP sonar. The data presented here from the *R/V Neil Armstrong* suggest that the *C/V Oleander*’s crossings with the OS38 will enable regular sampling not only of the deep-reaching Gulf Stream, but also of the upper part of the DWBC, providing valuable observations for studies of the AMOC’s cold and warm limb flows.

Data availability. Data are available through <http://marine.copernicus.eu> (altimetry) and <http://argo.whoiedu> (Argo) and <http://science.whoiedu/users/seasoar/peachadcp/>.

References

- Bane, J. M. Jr. & Dewar, W. K. Gulf Stream bimodality and variability downstream of the Charleston Bump. *Journal of Geophysical Research-Oceans* **93**(C6), 6695–6710 (1988).
- Miller, J. L. Fluctuations of Gulf Stream frontal position between Cape Hatteras and the Straits of Florida. *Journal of Geophysical Research* **99**(C3), 5057–5064, <https://doi.org/10.1029/93JC03484> (1994).
- Savidge, D. K. & Bane, J. M. Wind and Gulf Stream influences on along-shelf transport and off-shelf export at Cape Hatteras, North Carolina. *Journal of Geophysical Research* **106**(C6), 11,505–11,527 (2001).
- Andres, M. On the recent destabilization of the Gulf Stream path downstream of Cape Hatteras. *Geophysical Research Letters* **43**, <https://doi.org/10.1002/2016GL069966> (2016).
- Pickart, R. S. & Watts, D. R. Deep Western Boundary Current variability at Cape Hatteras. *Journal of Marine Research* **48**, 765–791 (1990).
- Gary, S. F., Lozier, M. S., Biastoch, A. & Böning, C. W. Reconciling tracer and float observations of the export pathways of Labrador Sea Water. *Geophysical Research Letters* **39**, L24606, <https://doi.org/10.1029/2012GL053978> (2012).
- Rhein, M., Kieke, D. & Steinfeldt, R. Advection of North Atlantic Deep Water from the Labrador Sea to the southern hemisphere. *Journal of Geophysical Research-Oceans* **120**, 2471–2487, <https://doi.org/10.1002/2014JC010605> (2015).
- Andres, M. *et al.* Stirring by deep cyclones and the evolution of Denmark Strait Overflow Water observed at Line W. *Deep Sea Research* **109**, 10–26, <https://doi.org/10.1016/j.dsr.2015.12.011> (2016).
- Le Bras, I. A., Yashayaev, I. & Toole, J. M. Tracking Labrador Sea Water property signals along the Deep Western Boundary Current. *Journal of Geophysical Research Oceans* **122**, 5348–5366, <https://doi.org/10.1002/2017JC012921> (2017).

10. Richardson, P. L. On the crossover between the Gulf Stream and the Western Boundary Undercurrent. *Deep Sea Research* **24**, 139–159 (1977).
11. Pickart, R. S. & Smethie, W. M. Jr. How does the Deep Western Boundary Current cross the Gulf Stream. *Journal of Physical Oceanography* **23**, 2602–2616 (1993).
12. Pickart, R. S. Interaction of the Gulf Stream and the Deep Western Boundary Current where they cross. *Journal of Geophysical Research* **99**(25), 155–25,164 (1994).
13. Thompson, J. D. & Schmitz, W. J. Jr. A limited-area model of the Gulf Stream: Design, initial experiments, and model/data intercomparison. *Journal of Physical Oceanography* **19**, 791–814 (1989).
14. Hogg, N. G. & Stommel, H. On the relation between the deep circulation and the Gulf Stream. *Deep Sea Research* **32**, 1181–1193, [https://doi.org/10.1016/0198-0149\(85\)90002-0](https://doi.org/10.1016/0198-0149(85)90002-0) (1985).
15. Saba, V. S. *et al.* Enhanced warming of the Northwest Atlantic Ocean under climate change, *Journal of Geophysical Research Oceans*, **120**, <https://doi.org/10.1002/2015JC011346> (2015).
16. Toole, J. M., Curry, R. G., Joyce, T. M., McCartney, M. & Peña-Molino, B. Transport of the North Atlantic Deep Western Boundary Current about 39N, 70W: 2004–2008. *Deep Sea-Research* **58**, 1768–1780, <https://doi.org/10.1016/j.dsr2.2010.10.058> (2011).
17. Toole, J. M., Andres, M., Le Bras, I. A., Joyce, T. M. & McCartney, M. S. Moored observations of the Deep Western Boundary Current in the NW Atlantic: 2004–2014. *Journal of Geophysical Research*, **122**, <https://doi.org/10.1002/2017JC012984> (2017).
18. Lozier, M. S. Overturning assumptions: Past, present, and future concerns about the ocean's circulation. *Oceanography* **28**(2), 240–251, <https://doi.org/10.5670/oceanog.2015.50> (2015).
19. Spall, M. A. Dynamics of the Gulf Stream/Deep Western Boundary Current Crossover. Part I: Entrainment and recirculation. *Journal of Physical Oceanography* **26**(10), 2152–2168 (1996).
20. Bower, A. S. & Hunt, H. D. Lagrangian observations of the Deep Western Boundary Current in the North Atlantic Ocean. Part I: Large-scale pathways and spreading rates. *Journal of Physical Oceanography* **30**(5), 764–783 (2000a).
21. Bower, A. S. & Hunt, H. D. Lagrangian observations of the Deep Western Boundary Current in the North Atlantic Ocean. Part II: The Gulf Stream-Deep Western Boundary Current Crossover. *Journal of Physical Oceanography* **30**(5), 784–804 (2000b).
22. Blanton, B. O. *et al.* Barotropic tides in the South Atlantic Bight. *Journal of Geophysical Research* **109**, C12024, <https://doi.org/10.1029/2004JC002455> (2004).
23. Meinen, C. S. & Luther, D. S. Structure, transport, and vertical coherence of the Gulf Stream from the Straits of Florida to the Southeast Newfoundland Ridge. *Deep Sea Research* **112**, 137–154, <https://doi.org/10.1016/j.dsr.2016.03.002> (2016).
24. Haines, S., Seim, H. & Muglia, M. Implementing quality control of high-frequency radar estimates and application to Gulf Stream surface currents. *Journal of Atmospheric and Oceanic Technology* **34**, 1207–1224, <https://doi.org/10.1175/JTECH-D-16-0203.1> (2017).
25. Rossby, T., Flagg, C. N., Donohue, K., Sanchez-Franks, A. & Lillibridge, J. On the long-term stability of Gulf Stream transport based on 20 years of direct measurements. *Geophysical Research Letters* **41**, 114–120, <https://doi.org/10.1002/2013GL058636> (2014).
26. Flagg, C., Schwartze, G., Gottlieb, E. & Rossby, T. Operating an acoustic Doppler current profiler (ADCP) aboard a container vessel. *Journal of Atmospheric and Oceanic Technology* **15**, 257–271 (1998).

Acknowledgements

This research was supported by NSF through OCE-1558521 and OCE-1332667 and by a grant from North Carolina to the Renewable Ocean Energy Program. We appreciate the efforts of Captain D. Bergeron and the *R/V Neil Armstrong* crew and gratefully acknowledge A. Simoneau and C. Seaton for their support capitalizing on the ship's observational capabilities during AR-15. We thank S. Haines, P.E. Robbins, and P. Taylor for help with the data sets and J. Churchill for help with the ADCIRC model.

Author Contributions

M.A. wrote the main manuscript text. M.M. led the analysis of the initial SVC-Cruise ADCP data and F.B. processed the AR-15 ADCP data. All authors contributed to the data interpretation and reviewed the manuscript.

Additional Information

Competing Interests: The authors declare no competing interests.

Publisher's note: Springer Nature remains neutral with regard to jurisdictional claims in published maps and institutional affiliations.



Open Access This article is licensed under a Creative Commons Attribution 4.0 International License, which permits use, sharing, adaptation, distribution and reproduction in any medium or format, as long as you give appropriate credit to the original author(s) and the source, provide a link to the Creative Commons license, and indicate if changes were made. The images or other third party material in this article are included in the article's Creative Commons license, unless indicated otherwise in a credit line to the material. If material is not included in the article's Creative Commons license and your intended use is not permitted by statutory regulation or exceeds the permitted use, you will need to obtain permission directly from the copyright holder. To view a copy of this license, visit <http://creativecommons.org/licenses/by/4.0/>.

© The Author(s) 2018